Journal of Nondestructive Evaluation (2020) 39:30
https://doi.org/10.1007/s10921-020-00675-4

Comparison of Experimental Measurements of Material Grain Size Using Ultrasound

Jie Zhang[1] · Yongfeng Song[2] · Xiongbing Li[2] · ChengHuan Zhong[3]

Received: 25 November 2019 / Accepted: 12 March 2020 / Published online: 18 March 2020

Abstract
Material grain size is related to metallic material properties and its elastic behaviour. Measuring and monitoring material grain size in material manufacturing and service is an important topic in measurement field. In this paper, three materials, i.e., aluminium 2014 T6, steel BS970 and copper EN1652, were chosen to represent materials with small, medium and large grain size, respectively. Various techniques of measuring material grain size were demonstrated and compared. These techniques include the measurements from material microstructure images, backscattered ultrasonic grain noise using a conventional transducer, longitudinal wave attenuation using ultrasonic arrays and shear wave attenuation using a lead zirconate titanate (PZT) plate. It is shown that the backscattered ultrasonic noise measurement and material attenuation measurement are complementary. The former is pretty good for weak scattering materials, e.g., aluminium, while the latter for materials with large grains, e.g., steel and copper. Consistent measured grain size from longitudinal and shear wave attenuations in steel and copper suggests that shear wave attenuation can be calculated from the measured longitudinal wave attenuation integrated with Stanke–Kino's model or Weaver's model, if there is a difficulty to either excite or capture shear waves in practice. The outcome of the paper expects to provide a further step towards the industrial uptake of these techniques.

Keywords Material grain size · Material attenuation · Ultrasound · Ultrasonic arrays

1 Introduction

Material grain size has significant effect on metallic material properties and its elastic behaviour. For example, fine-grained magnesium-based materials exhibit superplastic behaviour at high stain rates ($\geq 10^{-1}$ s^{-1}) or low temperatures (≤ 473 K) [1]; coarse-grained nickel-based alloys enhance yield strength by 60 MPa and creep resistance by 15° temperature gain [2]; the coarse grains in both columnar and equiaxed microstructures have presented a better corrosion behaviour than fine grain microstructures [3]. Measuring and monitoring material grain size in material manufacturing and service is hence an important topic in measurement field. There are many techniques used to achieve this. Traditionally, a small piece of specimen was taken from material and polished for microstructure imaging using either optical microscope or electron backscattering diffraction (EBSD) method [4]. Alternatively, the scattered ultrasound from material microstructure contains the grain size information and it can be indicated in ultrasound dispersion [5], attenuation [6–9] and backscattered grain noise [10–15].

Compared with the grain size measurement from either ultrasound dispersion or attenuation, that from backscatter grain noise has no requirement of parallel front-wall and back-wall surfaces and known wall thickness of a specimen. Instead more complicated statistical methods are required to combine the ultrasonic signals from different sets of grains at different probe spatial positions [10–15]. Margetan et al. [10] measured the root-mean-square (RMS) of noise amplitude as a function of material microstructure, termed as the figure of merit (FOM). Ghoshal et al. [13] developed a general backscattered grain noise model under multiple-scattering assumption and then simplified to the case for singly scattered response (SSR) [14] which is in agreement with the Margetan's model [10]. Hu and Turner extended the

✉ Jie Zhang
j.zhang@bristol.ac.uk

[1] Department of Mechanical Engineering, University Walk, University of Bristol, Bristol BS8 1TR, UK

[2] Key Laboratory for Traffic Safety on Track, Ministry of Education, Changsha, China

[3] Inductosense Limited, Unit 3, Kings Business Park, Kings Park Avenue, Bristol BS2 0TZ, UK

SSR model to the doubly scattered response (DSR) model [15] to include high order grain scattering. All above methods applied to normal incidence, pulse-echo inspection of weakly-scattering materials from either a planar or focused longitudinal wave transducer. From the practice point view, if the grain size measurement can be achieved by using other type of ultrasound probes, such as ultrasonic arrays and shear wave transducers, it will provide more choice for material grain size measurement in practice as well as add more inspection functions for each type of ultrasound probes.

The motivation of this paper is to demonstrate the various techniques of measuring material grain size and expect to provide a further step towards the industrial uptake of these techniques. Three materials, i.e., aluminium 2014 T6, steel BS970 and copper EN1652, were chosen to represent materials with small, medium and large grain size respectively and their material properties are shown in Table 1. The method of measuring grain size demonstrated in this paper includes the measurements from material microstructure images, backscattered ultrasonic grain noise using a conventional transducer and the SSR [14] and DSR models [15], longitudinal wave attenuation using ultrasonic arrays and shear wave attenuation using a lead zirconate titanate (PZT) plate. The last method is used to simulate a case of permanently attaching a low-cost sensor for structure health monitoring. It is noted that, in this paper, the grain size denotes the mean material grain diameter. The experimentally measured results from different methods were compared to demonstrate the measurement variability in practice. The measurement sensitivity and the application of measuring shear wave attenuation were discussed.

2 Measurements from Material Microstructure Images

The material microstructure images from the chosen materials were taken using either an optical microscope or the electron backscattering diffraction (EBSD) technique after proper preparation. In the preparation, the materials were first cut to a small specimen pieces and grounded using SiC papers with 1200 grit. Diamond slurries with particle sizes of 6 μm and 3 μm were then used to polish coarsely. Alumina slurries with particle sizes of 0.3 μm and 0.04 μm were finally used sequentially to polish all specimens. EBSD system composed of a FEI Quanta 650 FEG SEM and a NordlysMax2 EBSD detector was used to image the microstructure of the aluminium specimen at an indexing rate of 89.9%. However, for the other specimens, their surfaces were further etched before taking the micrographs. In the etching process, the steel specimen has done by the mixture of 5 g $C_6H_2(NO_2)_3OH$, 4 g $C_{18}H_{29}NaO_3S$, 5 mL H_2O_2 and 100 mL H_2O at 90 °C for ~ 45 s while the copper specimen was immersed in the mixture of 3 g Fe_2O_3, 2 mL HCl and 96 mL C_2H_6O for a minute. An Olympus BX53M optical microscope was used to obtain the microstructure images from these two specimens.

The measured microstructure image from the aluminium, steel and copper specimen is as shown in Fig. 1a–c, respectively. From these images, the material grain size on each specimen can be measured. In the measurement on the aluminium specimens, the grain size was calculated using the grain reconstruction method provided by software HKL CHANNEL5 (Oxford Instruments, UK). The 5-neighbor-extrapolation method was used to reduce the indexing rate effect. While, in the measurement on the other specimens, the linear intercept method [20] based on ASTM E112 [21] standard was used. To reduce measurement errors, five optical micrographs were randomly chosen on the detection cross-section of each specimen and the above procedures were used repeatedly to measure grain size. The measured grain sizes are as shown in Table 2. As expected, the smallest grain size is from the aluminium specimen while the largest one from the copper specimen.

3 Measurements from Backscattered Ultrasonic Grain Noise

Due to the randomness of backscattered ultrasonic signals from material structure, a single signal is not adequate to estimate the grain size, instead, a statistical quantity of the ensemble signals is used. In the measurement, a conventional ultrasonic scanning system is used to capture signals at various positions. The time-dependent spatial variance of the ensemble of all captured signals can be written as [14],

$$\Phi(t) = \frac{1}{N}\sum_{i=1}^{N} V_i^2(t) - \left[\frac{1}{N}\sum_{i=1}^{N} V_i(t)\right]^2, \quad (1)$$

where N is the number of captured signals and $V_i(t)$ is the amplitude of the ith captured signal. It can be seen that the spatial variance has no concern with the thickness of the specimen and the condition of the back-wall surface.

Specifically, considered various material grain sizes of the chosen specimens, the experiments were performed on the aluminium and steel specimens using a 10 MHz focused immersion transducer (Olympus V311-SU-F2.0-PTF), but on the copper specimen using a 5 MHz focused immersion transducer (Olympus V309-SU-F2.0-PTF). For the 10 MHz probe, the actual calibrated central frequency is 8.6 MHz, the calibrated focal length in water is 54.6 mm, the probe aperture size is 13.3 mm and this leads to the – 6 dB spot size as 0.7 mm. For the 5 MHz probe, the actual calibrated central frequency is 4.6 MHz, the calibrated focal length in water is 58.3 mm, the probe aperture size is 12.0 mm and this

Table 1 Elastic material properties of the chosen specimens

Material	Elastic property					
	c_{11} (GPa)	c_{12} (GPa)	c_{44} (GPa)	ρ (g/cm^3)	v_l (m/s)	v_t (m/s)
Aluminium [16]	108	63	29	2780	6408	3120
Steel [17]	229	134	117	7930	5850	3210
Copper [18, 19]	170	121	75	8984	4700	2286

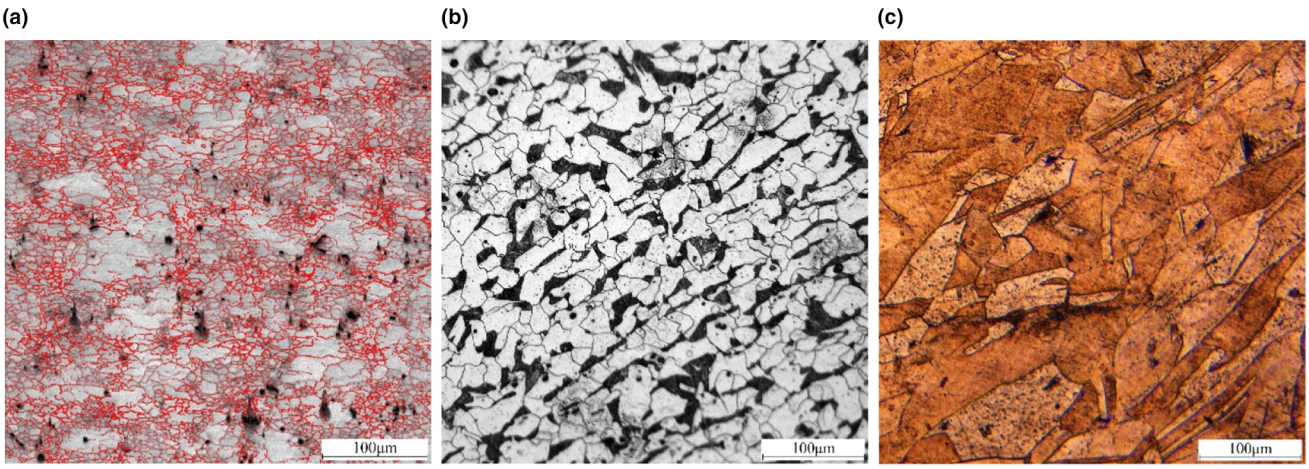

Fig. 1 The microstructure image from the; **a–c** aluminium, carbon steel and copper specimen

Table 2 Measured grain size from the chosen specimens using different methods

Material	Aluminium	Steel	Copper
Grain size (μm) measured from			
Image of microstructure	11.0 ± 0.6	21.2 ± 1.1	85.7 ± 4.7
Backscattered grain noise using the			
SSR method [13]	11 ± 1	37 ± 3	62 ± 4
DSR method [15]	11 ± 1	35 ± 3	52 ± 4
Longitudinal wave attenuation measured using ultrasonic arrays and the			
Stanke–Kino model [6]	46 ± 3	36 ± 2	80 ± 3
Weaver model [7]	46 ± 3	36 ± 2	80 ± 3
Shear wave attenuation measured using a shear wave PZT and the			
Stanke–Kino model [6]	56 ± 4	35 ± 2	78 ± 4
Weaver model [7]	56 ± 4	35 ± 2	78 ± 4

leads to the − 6 dB spot size as 1.6 mm. An Imaginant JSR-DPR300 pulser/receiver was used to excite the transducers and an acquisition system with an ADLink PCIe-9852 DAQ card was used to receive signals under a sampling frequency of 200 MHz. The above equipment and transducers were integrated into an automated immersion ultrasound scanning system and used to capture signals. In the experimental measurements, the transducers were maintained normally to the front-wall surface of the specimen. In the measurements for each specimen, 1024 signals were captured in a square region with scanning distance increment of 0.35 mm when using the 10 MHz transducer or 0.8 mm when using the 5 MHz transducer. Equation (1) was used to calculate the experimental spatial variance.

The predicted spatial variance from each specimen was obtained from the SSR [14] and DSR [15] models with the known material properties, known calibrated probe parameters and a group of testing grain sizes. The measured grain size is the one leading to the predicated spatial variance best fitting to the experimentally measured one. Figure 2a–c compare the best fitting results from the SSR and DSR models with the experimentally measured one for each specimen and the measured grain sizes from 10 repeated measurements are shown in Table 2. Comparing Fig. 2a–c, it is shown that the measured results on the aluminium specimens from the SSR and DSR models have a good agreement, however, for the results from the steel and copper specimens, DSR model shows better prediction than the SSR model. Comparing the measured grain sizes from the image of microstructure and the backscattered grain noise in Table 2, it can be seen that there is a good agreement for the aluminium specimens but some difference for the other specimens. There are some explanations and findings from the observations:

(1) The case of the aluminium specimen is closest to the model assumptions for material grain properties, i.e., single phase, cubic symmetry, untextured and equiaxed, and hence shows a good agreement.
(2) From Fig. 1b, it is shown that the steel specimen has two phases, i.e., ferrite and cementite, and this makes the SSR and DSR models for the single phase and constant density medium break down. The result from DSR model is somewhat better than the SSR model for such a strong scattering medium with two phases.
(3) It is noted that the copper specimen is slightly elongated as shown in Fig. 1c. The present results from the SSR and DSR models are closer to the short side of grain than the equivalent diameter, where the short side of the grains was re-measured as 54.5 ± 2.4 μm from the microstructure image. Although the backscattering models for elongated grains have been built [22, 23], they would be cumbersome to perform in the industrial application. It is suggested that at least 2 scans from orthogonal planes of the specimen are necessary to define an unknown elongated microstructure meanwhile there might be only one plane could be scanned for some large plates.
(4) In summary, the grain size measurements with the backscattered ultrasound grain noise models are suitable for some simple microstructures but need to be further developed for more complexed microstructures.

4 Measurements from Longitudinal Wave Attenuation Using Ultrasonic Arrays

The easiest way of using ultrasonic array to measure wave attenuation is to generate a normal incident plane wave relative to the back wall. The amplitude ratio between the first and second signals reflected from the back-wall is related to material attenuation. If both reflection signals are in the near field of the probe, the effect from wave beam spread and diffraction can be ignored [24]. This can be achieved experimentally by direct placing the array probe above a specimen or using a normal incidence immersion configuration. However, the former setup requires an accurate estimation of the reflection coefficient from the specimen-probe interface and it is difficult to know due to limit knowledge of array material properties and coupling uncertainty. The latter setup was hence used in here. In the frequency domain, the material longitudinal wave attenuation can be written as [25],

$$\alpha(f) = \frac{1}{2d} \ln\left(\frac{A_1(f)}{A_2(f)} R^2\right), \tag{2}$$

with a unit as Np/mm, where f is the frequency, d is the thickness of a specimen, and A_1 and A_2 is the amplitude of the signal from the first and second back-wall reflection. R is the reflection coefficient between the solid-water interface, and it can be written as [25],

$$R = \frac{Z_2 - Z_1}{Z_1 + Z_2}, \tag{3}$$

where Z_1 and Z_2 is the acoustic impedance of the specimen and water, respectively, and it is the product of the density and the longitudinal speed.

In order to obtain material attenuation at a wide frequency range, 3 ultrasonic array probes (manufactured by Imasonic, Besancon, France) with a central frequency of 5 MHz, 10 MHz and 15 MHz were used and their specifications are shown in Table 3. A commercial array controller (Micropulse MP5PA, Peak NDT, Ltd., Derby, UK) was used to capture the time-domain signals when all array elements were fired together to generate a normal incident plane wave. The captured data was then exported and processed using MATLAB (The MathWorks, Inc., Natick, MA) to calculate material attenuation using Eq. 2. The specimen fabricated by aluminium, steel and copper has a thickness of 31.5 mm, 30 mm and 26 mm, respectively. In the measurements, the standing-off distance of the array relative to the specimen top surface is 17 mm to get rid of the effect of the second front wall reflection on the second back-wall reflection.

As an example, Fig. 3a shows the time domain signal from the copper specimen captured using the 5 MHz array probe. In Fig. 3a, the signals from the first and second back-wall reflections can be identified by their arrival times and are shown as the blue and red signals. Figure 3b compares the frequency spectrums of the back-wall signals obtained using the 5 MHz, 10 MHz and 15 MHz array probes from the copper specimen. Note that the amplitude in each spectrum pair is normalized to its own maximum. As shown, the amplitude ratio between the first and second back-wall signals increases when the probe frequency increases due to material attenuation. Figure 3c compares the experimentally measured longitudinal wave attenuations from 3 chosen materials using 3 array probes, as shown as different symbols with different colors. The material grain sizes were finally measured by comparing the experimentally measured attenuation and predicted ones using Stanke–Kino model [6] and Weaver model [7]. The measured grain size is the one leading to the predicted results best fit with the experimentally measured ones. The best fit curves are shown in Fig. 3c as the solid curves from Stanke–Kino model and the solid curves with cross symbols from Weaver model. As shown, the measurement results using Stanke–Kino model is nearly identical to those from Weaver model. The measured grain sizes based on 10 repeatedly measurements are shown in Table 2 in which there is a good agreement between the measurements from the ultrasonic arrays and the conventional probes using the

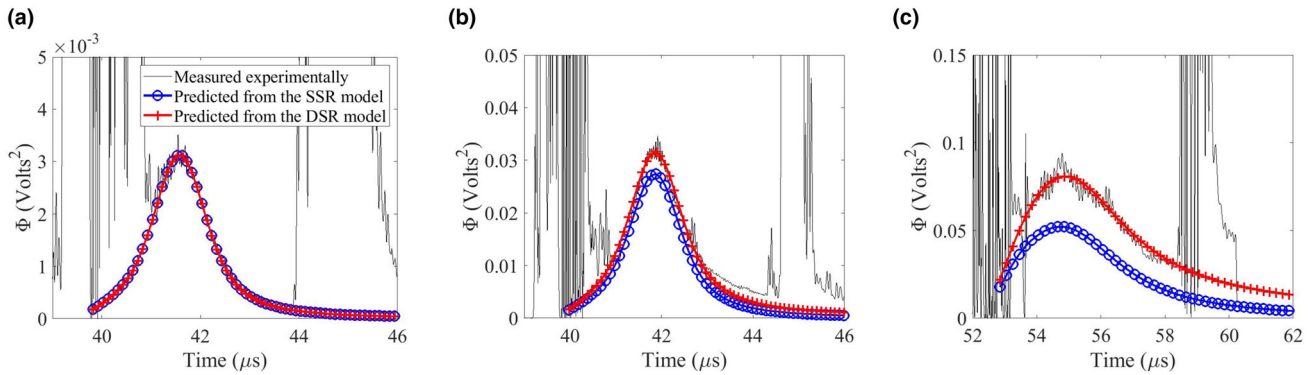

Fig. 2 The spatial variance of the backscattered ultrasound grain noise signals from (**a**); **a**–**c** aluminium, steel and copper specimen. Note that, in each figure, the solid black line is from the experimental measurements, the blue line with circle symbols is predicated using the SSR model and the red line with cross symbols is done using the DSR model (Color figure online)

Table 3 Specification of the array transducer used in the experimental measurements

Number of element N	Central frequency (MHz)	Element width (mm)	Element pitch (mm)	Array aperture size (mm)
128	5	0.1	0.3	40
128	10	0.1	0.3	40
64	15	0.20	0.21	13.23

backscattered grain noise method for the steel specimen but not for the aluminium and copper specimens. It is noted that the effects of grain size distribution and grain elongation are ignored in both Stanke–Kino model [6] and Weaver model [7]. There are some explanations and findings from the observations:

1. It is shown that the attenuation measurement in aluminium is less accurate than that in steel and copper. This means that the attenuation in aluminium is too low to be used to calculate material grain size in practice;
2. It should be noted that the effects of cementite on the ultrasonic scattering in steel is ignored and this leads to larger measured grain size than those from the microstructure images, but a good agreement with those from the ultrasound backscattering grain noise methods;
3. It is shown that the measured grain sizes from the copper specimens are close to the equivalent diameters measured from the microstructure images.

5 Measurements from Shear Wave Attenuation Using a PZT Plate

Here, a shear wave PZT plate was used to measure material shear wave attenuation to expect to achieve better measurement sensitivity. In the measurements, a PZT plate PIC 255 (fabricated by PI Ceramic, Germany) with a size of 4 mm by 7 mm and a thickness of 0.18 mm was bonded above a specimen using epoxy adhesive. The first resonance frequency of the PZT plate is 5 MHz. Due to the thin thickness of the PZT plate and thin and consistent bond condition, the reflection coefficient from the specimen-PZT plate interface approximates as same as that from the specimen-air interface ($R = 1$). The specimens were fabricated using aluminium, steel and copper and have a thickness of 15 mm. A tone-burst signal with a central frequency of 5 MHz and a bandwidth of 100% fraction at − 20 dB was loaded on the PZT. As an example, Fig. 4a, b show the time domain signal and its frequency spectrum from the copper specimen, respectively. Figure 4c compares the measured shear wave attenuation from various specimens. As expected, they are higher than the longitudinal wave attenuation as shown in Fig. 3c. The material grain sizes were measured by comparing the experimentally measured attenuation (shown as symbols) and predicted ones using Stanke–Kino model [6] and Weaver model [7]. The best fit predicted attenuation curves are shown in Fig. 4c as the solid curves from Stanke–Kino model and the solid curves with cross symbols from Weaver model. Again, the measurement results using Stanke–Kino model is nearly identical to those from Weaver model. The measured grain sizes are listed in Table 2. From Table 2 it is shown that there is a good agreement between the measurements from the longitudinal wave and the shear wave for the steel and copper specimens but not for the aluminium specimens. This again indicates the attenuation in aluminium is too low to be used to calculate material grain size in practice.

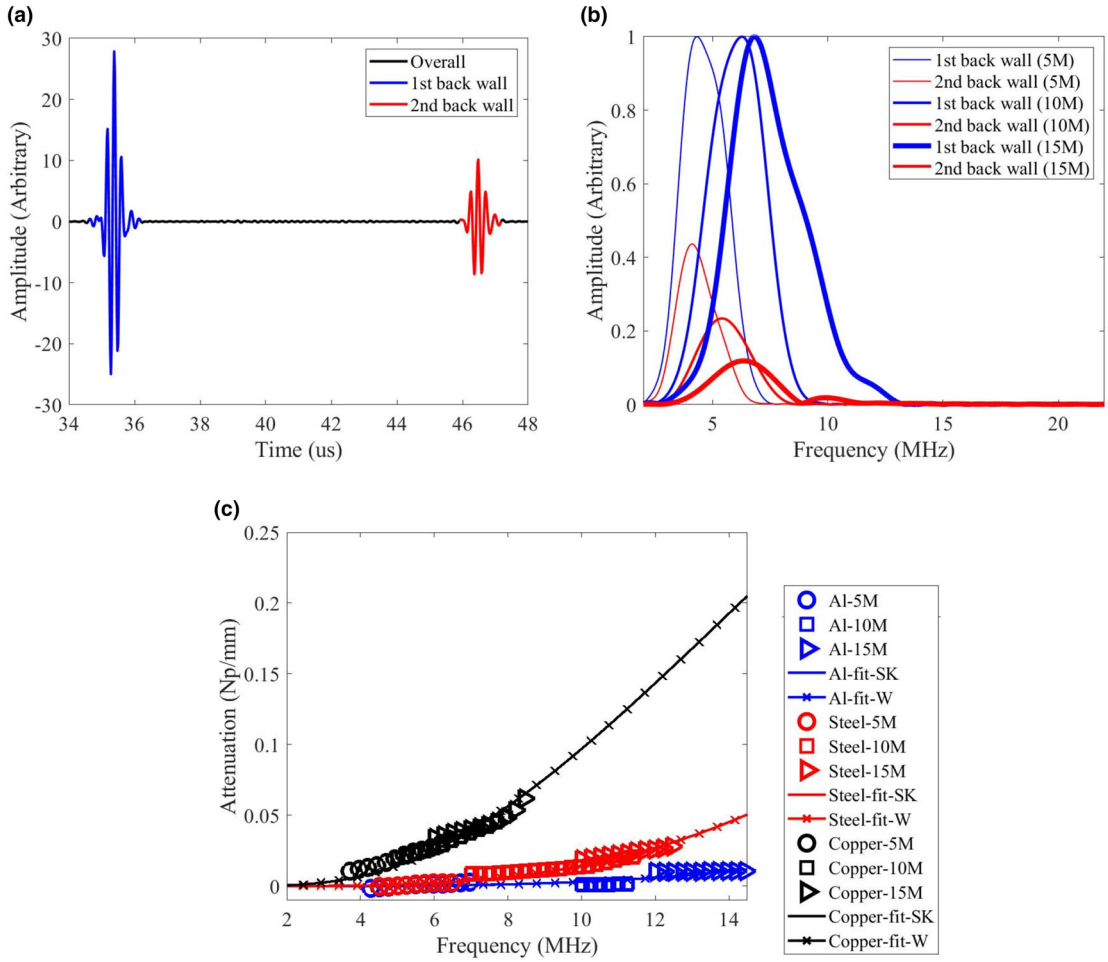

Fig. 3 Experimental results from the measurements using ultrasonic arrays. **a** An example of time domain signal captured using the 5 MHz array from the copper specimen, **b** the comparison of the frequency spectrum of the back-wall signals from the copper specimen and captured using various array probes and **c** the comparison of measured longitudinal wave attenuation using various array probes on different specimens

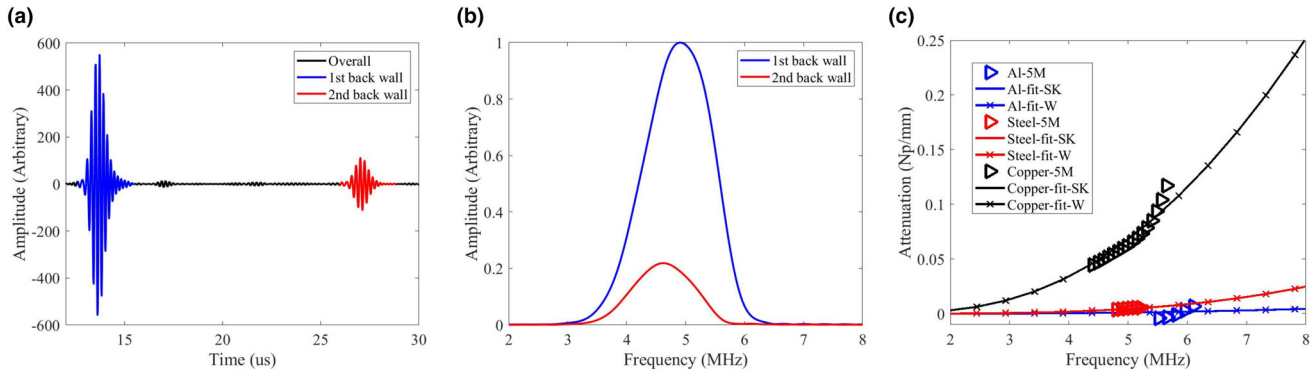

Fig. 4 Experimental results obtained from a 5 MHz shear wave PZT plate; **a**, **b** the time domain back-wall signals and their spectrums from the copper specimen and **c** the comparison of measured shear wave attenuation on different materials

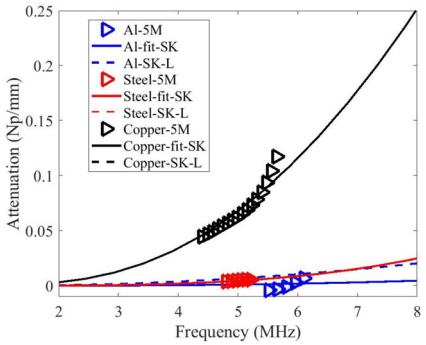

Fig. 5 The comparison of measured shear wave attenuation using different methods for various materials

6 Discussion

6.1 Shear Wave Attenuation Measurement

In practice, the generation of shear wave using a conventional probe requests special coupling gel while either oblique incident in water or a coupling wedge is required in an ultrasonic array system. This limits shear wave attenuation measurement in practice. The consistent of the measured grain sizes from longitudinal wave and shear wave for the steel and copper specimens indicates that shear wave attenuation can be worked out from longitudinal attenuation through the measured grain size and proper models, for example, the Stanke–Kino model [6] and the Weaver model [7]. Figure 5 compares the measured shear wave attenuation using this method (the dashed lines) and the direct best fit curves (the solid lines) from the measurements using the shear wave PZT (the symbols). Again, there is a good agreement for the steel and copper specimens, but 0.015 Np/mm at 8 MHz for the aluminium specimens. This indicates the proposed method works for the steel and copper specimens but not the aluminium specimens.

6.2 Measurement Sensitivity

Comparing the best fit curves as shown in Figs. 3c and 4c, it can be seen that, the attenuation measurement sensitivity is higher in materials with large grains than those with small grains and it increases with frequency. It also suggests that the attenuation in aluminium is more difficult to be measured compared with the other materials.

Figure 6a, b compares the predicted material attenuation as a function of grain size for the 3 chosen material properties at 5 MHz and 8 MHz. Again, it is shown that high measurement sensitivity is happened for large grain size at high frequency and the measurement from shear wave shows better sensitivity than longitudinal wave. When grain size is less than 20 μm, the sensitivity is poor and hence the grain size in aluminium is difficult to be measured from material attenuation. However, for the other materials, the measurement sensitivity is good. For example, at 5 MHz, the measurement sensitivity for a grain with size ranging 40 μm to 60 μm in steel is 0.00014 Np/(mm μm) and 0.00052 Np/(mm μm) for longitudinal and shear wave respectively. The measurement sensitivity for a grain with size ranging 90 μm to 100 μm in copper is 0.00033 Np/(mm μm) and 0.0017 Np/(mm μm) for longitudinal and shear wave respectively.

7 Conclusion

The variability of material grain size measurement demonstrates an acceptable measurement accuracy compared with the measurements from material microstructure images. It is shown that the backscattering ultrasound noise method and material attenuation method for material grain size measurement are complementary. The former is pretty good for all chosen materials and the latter for materials with large grains, e.g., steel and copper. The DSR model shows better prediction than the SSR model for materials with large grains. Materials with large grains and measured at high frequency and using shear wave attenuation can achieve better sensitivity in grain size measurement. Consistent measured

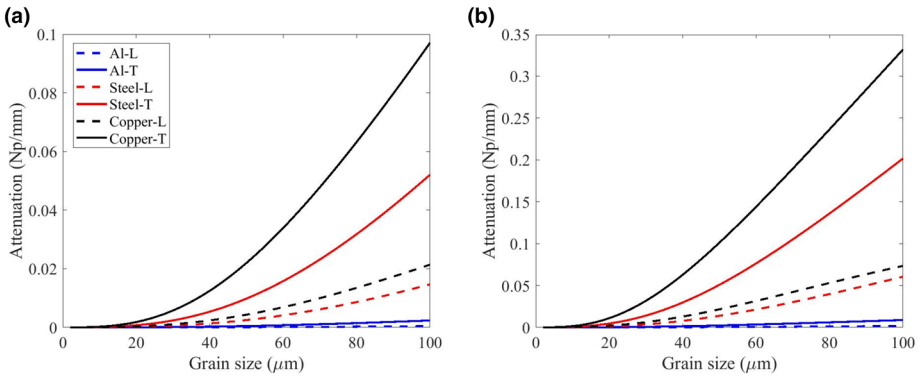

Fig. 6 Predicted material attenuation as a function of grain size from the materials with the properties listed in Table 1 and using the Stanke–Kino model at; **a**, **b** 5 MHz and 8 MHz

grain size from longitudinal and shear wave attenuations in steel and copper suggests that shear wave attenuation can be calculated from the measured longitudinal wave attenuation integrated with the Stanke–Kino's model or the Weaver's model, if there is a difficulty to either excite or capture shear waves in practice.

Acknowledgements This work was supported by Royal Society international exchanges cost share award with NSFC (Grant No. IE160986). This work was also supported through the core research programme within the UK Research Centre in NDE (RCNDE) funded by EPSRC (Grant No. EP/L022125/1) and the National Natural Science Foundation of China (Grant No. 51575541).

References

1. Kubota, K., Mabuchi, M., Higashi, K.: Review processing and mechanical properties of fine-grained magnesium alloys. J Mater Sci **34**, 2255–2262 (1999)
2. Cui, C.Y., Gu, Y.F., Yuan, Y., Osada, T., Harada, H.: Enhanced mechanical properties in a new Ni–Co base superalloy by controlling microstructures. Mater. Sci. Eng. A **528**, 5465–5469 (2011)
3. Osório, W.R., Freire, C.M., Garcia, A.: The role of macrostructural morphology and grain size on the corrosion resistance of Zn and Al castings. Mater. Sci. Eng. A **402**, 22–32 (2005)
4. Humphreys, F.J.: Characterisation of fine-scale microstructures by electron backscatter diffraction (EBSD). Scr. Mater. **51**, 771–776 (2004)
5. Every, A.G., Maznev, A.A.: Dispersion of an acoustic pulse passing through a large-grained polycrystalline film. J. Acoust. Soc. Am. **131**, 4491–4499 (2012)
6. Stanke, F.E., Kino, G.S.: A unified theory for elastic wave propagation in polycrystalline materials. J. Acoust. Soc. Am. **75**, 665–681 (1984)
7. Weaver, R.L.: Diffusivity of ultrasound in polycrystals. J. Mech. Phys. Solids **38**, 55–86 (1990)
8. Kube, C.M., Turner, J.A.: Acoustic attenuation coefficients for polycrystalline materials containing crystallites of any symmetry class. J. Acoust. Soc. Am. **137**, EL476-EL482 (2015)
9. Li, X., Song, Y., Liu, F., Hu, H., Ni, P.: Evaluation of mean grain size using the multi-scale ultrasonic attenuation coefficient. NDT&E Int. **72**, 25–32 (2015)
10. Margetan, F.J., Gray, T.A., Thompson, R.B.: A technique for quantitatively measuring microstructurally induced ultrasonic noise. In: Thompson, D.O., Chimenti, D.E. (eds.) Review of Progress in QNDE, vol. 10, pp. 1721–1728. Plenum Press, New York (1991)
11. Han, K.Y., Thompson, R.B.: Ultrasonic backscattering in duplex microstructures theory and application to titanium alloys. Metall. Mater. Trans. A **28**, 91–104 (1991)
12. Rose, J.H.: Ultrasonic backscatter from microstructure. In: Thompson, D.O., Chimenti, D.E. (eds.) Review of Progress in QNDE, 11, pp. 1677–1684. New York, Plenum Press (1992)
13. Ghoshal, G., Turner, J.A., Weaver, R.L.: Wigner distribution of a transducer beam pattern within a multiple scattering formalism for heterogeneous solids. J. Acoust. Soc. Am. **122**, 2009–2021 (2007)
14. Ghoshal, G., Turner, J.A.: Diffuse ultrasonic backscatter at normal incidence through a curved interface. J. Acoust. Soc. Am. **128**, 3449–3458 (2010)
15. Hu, P., Turner, J.A.: Contribution of double scattering in diffuse ultrasonic backscatter measurements. J. Acoust. Soc. Am. **137**, 321–334 (2015)
16. Pierce, D.T., Nowag, K., Montagne, A., Jimenez, J.A., Witting, J.E., Ghisleni, R.: Single crystal elastic constants of high-manganese transformation-and twinning-induced plasticity steels determined by a new method utilizing nanoindentation. Mater. Sci. Eng. A **578**, 134–139 (2013)
17. Du, H., Turner, J.A.: Ultrasonic attenuation in pearlitic steel. Ultrasonics **54**, 882–887 (2014)
18. Thompson, R.B., Smith, J.F., Lee, S.S., Johnson, G.C.: A comparison of ultrasonic and X-ray determinations of texture in thin Cu and Al plates. Metall. Mater. Trans. A **20**, 2431–2447 (1989)
19. Levy, M., Bass, H.E., Stern, R.R.: Handbook of Elastic Properties of Solids, Liquids and Gasses. Academic Press, London (2001)
20. Abrams, H.: Grain size measurement by the intercept method. Metallography **4**, 59–78 (1971)
21. ASTM E112–10: Standard Test Method for Determining Average Grain Size. American Society for Testing and Materials, West Conshohocken (2010)
22. Lobkis, O.I., Rokhlin, S.I.: Characterization of polycrystals with elongated duplex microstructure by inversion of ultrasonic backscattering data. Appl. Phys. Lett. **96**, 161905 (2010)
23. Arguelles, A.P., Kube, C.M., Hu, P., Turner, J.A.: Mode-converted ultrasonic scattering in polycrystals with elongated grains. J. Acoust. Soc. Am. **140**, 1570–1580 (2016)
24. Rogers, H., Van Buren, A.L.: An exact expression for the Lommel diffraction correction integral. J. Acoust. Soc. Am. **55**, 724–728 (1974)
25. Krautkramer, J., Krautkramer, H.: Ultrasoinc Testing of Materials. Springer, New York (2003)